Pergamon

0301-9322(95)00013-5

*Int. J. Multiphase Flow* Vol. 21, No. 4, pp. 693–704, 1995

0301-9322/95 $9.50 + 0.00

# AN EXPERIMENTAL STUDY OF VISCOUS RESUSPENSION IN A PRESSURE-DRIVEN PLANE CHANNEL FLOW

U. SCHAFLINGER, A. ACRIVOS† and H. STIBI

Institut für Strömungslehre und Wärmeübertragung, Technische Universität Wien, Karlsplatz 13, 1040 Wien, Austria

*(Received 2 October 1994; in revised form 8 February 1995)*

**Abstract**—Resuspension is a process by which an initially settled layer of heavy particles in contact with a clear fluid above it is set into motion by a laminar shear flow. Experiments were performed in a fully-developed Hagen–Poiseuille stratified channel flow with a clear fluid overlying a suspension, in order to measure the pressure drop and the particle velocity at the suspension—clear fluid interface as functions of the well-mixed particle volume fraction $\phi_s$ and a Shields number $\kappa$ which is a measure of the relative importance of viscous forces to those of gravity. It was found that, for a fixed feed concentration, the measured pressure drop coefficient $K$ decreased abruptly at $\kappa \sim 0.006$ and attained values which were significantly lower than those predicted theoretically. At the same time interfacial waves were observed which eventually became very strong. A further increase in $\kappa$ led to wave destruction and the appearance of clouds of detached particles moving relatively rapidly above the original interface. In this range the pressure drop coefficient increased and reached a value almost independent of $\kappa$. The intensity of wave breaking then lessened but remained significant. The measured particle velocity at the interface showed good agreement with the theory for small values of $\kappa$. At larger values, however, the observed particle velocity at the interface was up to several times larger than that predicted due to the existence of a detached particle layer that moved very rapidly. Finally, an additional flow instability was observed, a ripple type of instability, when the bottom of the channel was covered by a monolayer of particles.

*Key Words:* resuspension, laminar stratified flow

## 1. INTRODUCTION

When a clear fluid flows above an initially settled bed of heavy, non-Brownian particles, at least part of the sediment layer will resuspend, even at low Reynolds numbers. The physics of this phenomenon, termed viscous resuspension, has been described in several articles (Leighton & Acrivos 1987a, b; Acrivos 1993). In addition, a number of uni-directional flows such as a plane Couette flow (Leighton & Acrivos 1986), a plane film flow, a 2-D Hagen–Poiseuille channel flow (Schaflinger *et al.* 1990) and a quasi-unidirectional resuspension flow (Nir & Acrivos 1990; Kapoor & Acrivos 1995), which occurs in inclined gravity settling, were investigated based on a theoretical model developed by Leighton & Acrivos (1986). Recently, Zhang & Acrivos (1994) extended the model to study viscous resuspension in fully developed laminar pipe flows where the flow is completely three-dimensional.

Measurements of the resuspension height (Leighton & Acrivos 1986; Schaflinger *et al.* 1990) are in overall agreement with the theoretical predictions. The data show, however, considerable scatter which was attributed both to the difficulties in performing the measurements and to the presence of interfacial waves. Zhang *et al.* (1992) carried out a linear stability analysis and found that a 2-D Hagen–Poiseuille resuspension flow is almost always unstable to interfacial waves. In performing this analysis, these authors assumed that the particle concentration was uniform throughout the resuspension layer, which is justified by the base-state results even for moderate flow-rates of the clear liquid. A subsequent numerical study of this problem (Schaflinger 1994) revealed, however, the linear stability of the system is quite sensitive to the value of this uniform concentration. This is due to the fact that, since the concentration within the suspension layer is typically always near

†Present address: City College of New York, T-1M, 140th Street at Convent Avenue, New York, NY 10031, U.S.A.

the maximum value at which the effective viscosity of the suspension becomes infinite, even small variations of the concentration strongly influence this effective viscosity and therefore the stability of the flow. Zhang *et al.* (1992) and Schaflinger (1994) also discovered the existence of two different convective instabilities: relatively long and short waves, which coexist within a certain range of parameters (Schaflinger 1994).

In this paper we report the results of resuspension experiments which were performed in a pressure-drive two-dimensional Hagen–Poiseuille channel. Here, instead of measuring the resuspension height (Leighton & Acrivos 1986; Schaflinger *et al.* 1990), we focused our attention to the pressure drop which is relatively easy to measure and is also of great practical interest, e.g. in oil prospecting (Unwin & Hammond 1994). In addition, we were able to determine from video recordings the particle velocities at the interface. We found that, if the Shields number $\kappa$ was small, the pressure drop coefficient $K$ was in all cases, slightly larger than predicted theoretically (Schaflinger *et al.* 1990), and that the observed particle velocity at the weakly wavy interface was in good agreement with corresponding theoretical results by Schaflinger *et al.* (1990). Moreover, with the well-mixed particle concentration $\phi_s$ held constant, $K$ was found to decrease abruptly at $\kappa \sim 0.006$ and to attain values surprisingly lower than those predicted by theory. At the same time the interfacial waves became very strong and eventually, by breaking, released clouds of detached particles moving above the original interface. Under those conditions, the measured particle velocity at the interface was several times larger than calculated. A further increase in $\kappa$ raised the pressure drop coefficient $K$ which eventually reached a value almost independent of $\kappa$.

Finally, when the bottom of the channel was covered by a monolayer of these same spherical particles, a ripple type instability was observed during the experiments. The wavelength of this instability was always equal to approximately 10 particle diameters and did not change with increasing flow rate of the clear liquid.

## 2. THEORETICAL BACKGROUND

Consider a suspension of heavy spheres of uniform size and density resuspended in a 2-D Hagen–Poiseuille channel, as depicted in figure 1.

The symbol $h_0$ denotes the height of the sediment which would be attained if the flow were stopped and the particle layer had reached its maximum volume concentration $\phi_0 \sim 0.58$. The position of the top of the resuspended layer in the presence of a laminar shear flow with velocity $U(z)$ is denoted by $h_t$. $Q$ is the volumetric flux of clear liquid per unit depth, $\phi_s$ refers to the particle volume fraction if the suspension were to be well-mixed, $\mu$ is the viscosity, $\rho$ the density and $\nu$ the kinematic viscosity. The subscript m refers to the particle–fluid mixture within the resuspended layer with both the viscosity $\mu_m$ and the density $\rho_m$ being functions of the local particle concentration $\phi(z)$. Where necessary within the text, the subscripts 1 and 2 will distinguish between the clear fluid and particle properties, respectively. Furthermore, the symbol $\boldsymbol{g}$ refers to the gravitational constant. Finally, the total height of the 2-D duct is denoted by $2B$.

For uni-directional fully-developed laminar flows, the particle flux due to a gradient in concentration and a gradient in the shear stress $\tau$ is balanced by the particle flux due to gravity, hence

$$\frac{2\phi a^2 g\epsilon}{9\nu_1} f(\phi) + \dot{\gamma}(z) a^2 \tilde{D} \frac{\mathrm{d}\phi}{\mathrm{d}z} + \dot{\gamma}(z) a^2 \tilde{D} \frac{1}{\tau} \frac{\mathrm{d}\tau}{\mathrm{d}z} = 0, \qquad [1]$$

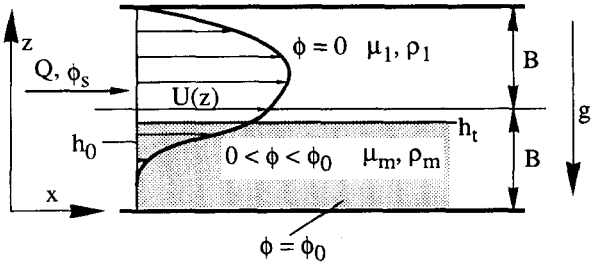


Figure 1. Schematic of a 2D Hagen–Poiseuille flow indicating the notation.

with the diffusion coefficients given as (Leighton & Acrivos 1987b)

$$\hat{D} = \frac{1}{3}\phi^2\left(1 + \frac{1}{2}e^{8.80\phi}\right), \tag{2}$$

and

$$\tilde{D} = 0.6\phi^2. \tag{3}$$

In [1] $f(\phi)$ refers to the hindrance function.

Also, the shear rate $\dot{\gamma}$ is given by:

$$\dot{\gamma} = \tau(z)/\mu_m(z), \tag{4}$$

with the effective viscosity written as (Leighton & Acrivos 1986)

$$\mu_r = \frac{\mu_m}{\mu_l} = \left(1 + \frac{1.5\phi}{1 - \phi/\phi_0}\right)^2, \ \phi_0 \sim 0.58. \tag{5}$$

Finally, the symbol $\epsilon$ denotes the relative density difference

$$\epsilon = (\rho_2 - \rho_l)/\rho_l. \tag{6}$$

In what follows, we shall neglect the last term in [1] since, in this case, shear-induced migration due to a gradient of concentration dominates. The system of equations governing the velocity and particle concentration profiles contain two parameters: the well-mixed particle concentration $\phi_s$ and a modified Shields number

$$\kappa = 9\nu_l Q/16B^3 g\epsilon, \tag{7}$$

which is a measure of the strength of viscous forces relative to those of gravity. $\kappa$ is related to the channel Reynolds number via

$$\mathrm{Re} = \kappa\epsilon\frac{16B^3 g}{9\nu_l^2}. \tag{8}$$

It is interesting to note that the particle radius $a$ does not enter into the picture. This fact was confirmed by earlier experiments (Leighton & Acrivos 1986; Schaflinger *et al.* 1990).

Equation [1], together with the equations of motion and continuity and the appropriate boundary conditions, has to be solved numerically. Schaflinger *et al.* (1990) obtained such numerical results for, *int.al.* the dimensionless pressure drop coefficient $K$ in a 2-D Hagen–Poiseuille channel defined according to

$$\Delta p = p_{in} - p_{out} = KL\mu_l Q/2B, \tag{9}$$

where $L$ is the total length of the duct.

## 3. EXPERIMENTAL SET-UP

A sketch of the experimental apparatus is shown in figure 2. The acrylic test section consisted of a rectangular duct of width 80 mm, height 10 mm and total length $L = 1$ m. The conduit had inlet ports for both the sediment and the clear fluid and one outlet port for the suspension. The concentration $\phi_s$ of the heavy, spherical particles (polystyrene beads with either radius $a = 410\,\mu$m and density $\rho_2 = 1031$ kg/m$^3$ or radius $a = 185\,\mu$m and density $\rho_2 = 1043$ kg/m$^3$) was measured by means of a laser beam, a transparent flow-cell, a photo diode and a voltage meter, a technique which was used in the past for similar measurements, e.g. Borhan (1988). Since the particles were opaque, concentration measurements were limited to values of $\phi_s$ below approximately 8%. Upon leaving the concentration measuring unit, the suspension flowed into an inclined settler where the particles were separated from the fluid (water–ethanol mixture, $\rho_l = 963$ kg/m$^3$; $\nu_l = 2.86 \times 10^{-6}$ m$^2$/s). Pump 2 conveyed the highly concentrated suspension into tank 2, from where a sediment with particle concentration close to $\phi_0 \sim 0.58$ was forced back into the resuspension channel by means of an adjustable pressure. Pump 3 returned any surplus of clear fluid into the settler. Purified liquid flowed from the settler into tank 1, where air bubbles could

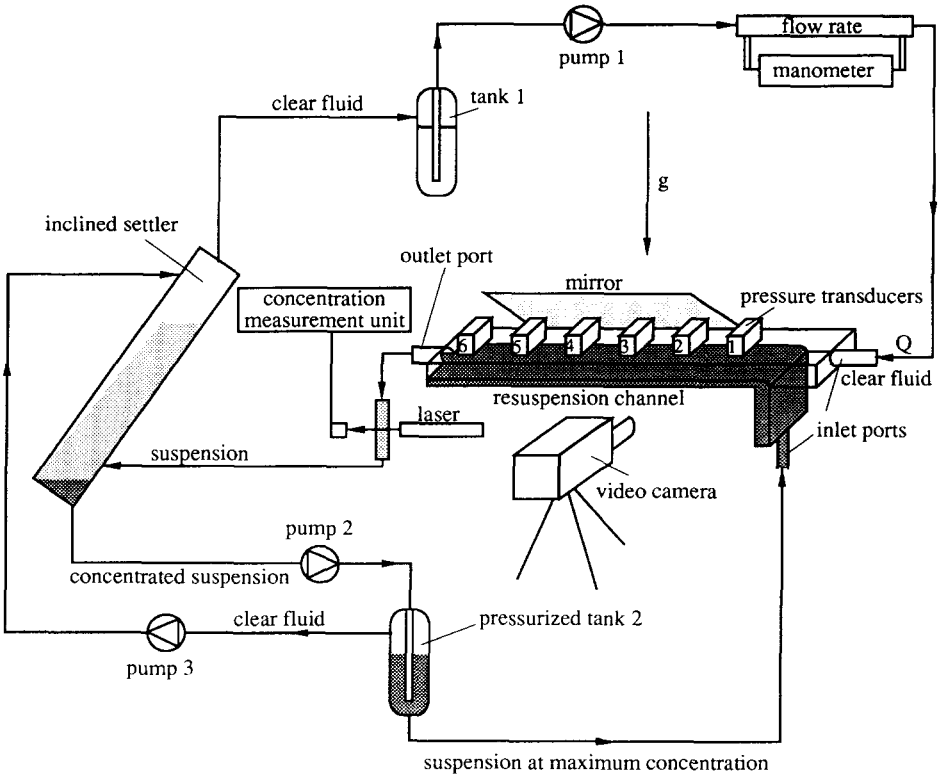


Figure 2. Experimental set-up.

escape. Finally, by means of pump 1 the clear fluid was made to flow through a manometer before it entered the resuspension conduit. The reading of the manometer was related to the flow rate of the clear liquid†). In all experiments the temperature was controlled and kept constant at $21 \pm 0.5^{\circ}$C.

By setting the flow rate of the clear liquid and the pressure difference between tank 2 and the channel, it was possible to achieve a fully developed, equilibrium resuspension flow within a short time.

For sedimenting suspensions, an estimate for the entrance length $L_\phi$, required for the establishment of a fully developed particle concentration profile, can be obtained readily by balancing the convective flux and that due to sedimentation. This is because, when a well-mixed but dilute suspension of heavy particles enters the channel, the flux due to shear-induced diffusion is negligible at first and becomes important only at a later stage, i.e. when the flow has already segregated into a pure liquid and a concentrated suspension. Consequently

$$\frac{Q}{BL_\phi} \sim \frac{a^2 g \epsilon}{B v_1} \quad \text{or} \quad L_\phi \sim \kappa \frac{B^3}{a^2}. \qquad [10]$$

This is in contrast to the case of neutrally buoyant particles, where a balance between the convective flux and that due to shear induced diffusion leads to the estimate

$$L_\phi \sim \frac{B^3}{a^2}.$$

In all the experiments, the value of $L_\phi$ given by [10] was much smaller than the total length of the channel $L$, since $\kappa B^3/a^2$ never exceeded approximately 5 cm.

Six pressure transducers, 10 cm apart, were mounted on top of the channel. In this manner the pressure drop could be monitored at five different positions along the channel. In addition, by

†The additional liquid fed into the channel by the highly concentrated suspension was, in all experiments, negligibly small compared to the total clear liquid flow.

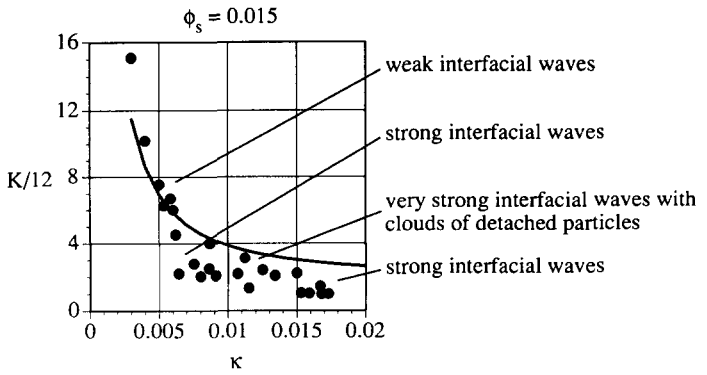


Figure 3. Measured pressure drop coefficient $K/12$ vs $\kappa$ for $0.01 < \phi_s < 0.02$ (water–ethanol mixture, $\rho_1 = 963\ \mathrm{kg/m^3}$; $\nu_1 = 2.86 \times 10^{-6}\ \mathrm{m^2/s}$; polystyrene beads with radius $a = 185\ \mu\mathrm{m}$ and density $\rho_2 = 1043\ \mathrm{kg/m^3}$) and comparison with theory (Schaflinger *et al.* 1990).

means of a mirror, the side view, which gives the top of the interface of the resuspension flow, and the top view, which gives the particle velocity at the interface, could be simultaneously recorded on a video. Thus, it was possible to measure the particle velocities at the interface and to study the instabilities of the flow.

## 4. EXPERIMENTAL RESULTS

### *(a) Pressure drop measurements*

In earlier experiments, Leighton & Acrivos (1986) and Schaflinger *et al.* (1990) measured $h_1$ as a function of the Shields number and of $\phi_s$. The data, however, exhibited large scatter because, at least in the system studied by Schaflinger *et al.* (1990), interfacial waves made it difficult to determine the actual resuspension height. In the present investigation the measured data for the height of the interface showed very much similar scatter as the previous experiments (Leighton & Acrivos 1986; Schaflinger *et al.* 1990). Thus, we focused our attention on the pressure drop which is relatively easy to measure and is less sensitive to local disturbances.

We checked the pressure drop at the beginning of the experiments for a laminar 2D Hagan–Poiseuille channel flow without particles and found that the pressure drop coefficient $K$ was in excellent agreement with the theoretically predicted value of 12. Also, it turned out that in all the experiments the pressure gradient was essentially constant along the channel. Only in the case of relatively small volume concentrations, $\phi_s < 0.035$, were fluctuations noticed at larger $\kappa$.

Figures 3–9 show the measured pressure drop coefficient $K$ as a function of $\kappa$ for different values of $\phi_s$ (water–ethanol mixture, $\rho_1 = 963\ \mathrm{kg/m^3}$; $\nu_1 = 2.86 \times 10^{-6}\ \mathrm{m^2/s}$; polystyrene beads with radius $a = 185\ \mu\mathrm{m}$ and density $\rho_2 = 1043\ \mathrm{kg/m^3}$)†. In all cases, $K$ was somewhat larger than expected by theory if $\kappa$ was small. In this range we observed interfacial waves with rather small amplitudes which were of the order of a few particle diameters. Increasing $\kappa$ always led to more vigorous instabilities and to an abrupt decrease of $K$ below the theoretical predictions at $\kappa \sim 0.006$. For $\kappa$ between 0.006 ($\phi_s \sim 0.015$) and 0.007 ($\phi_s \sim 0.075$) the waves were very strong with an amplitude of about 1/4 of the channel's height. An even further increase of $\kappa$ caused disintegration of the waves and generated clouds of detached particles moving above the original interface (figure 12). In all cases, the intensity of wave disintegration lessened when $\kappa > 0.013$.

It turned out to be difficult to experiment for relatively small concentration $\phi_s$ and larger $\kappa$ because the presence of interfacial waves led to a significant variation in $\phi_s$ as it was being measured after the outlet port of the channel. For $\phi_s \sim 0.015$ this variation was about 30%, 20% for $\phi_s \sim 0.025$, 10% for $\phi_s \sim 0.035$ and less than 10% for all higher concentrations. Together with the fact that the pressure gradient also varied along the channel, the data in figures 3 and 4 are highly uncertain at the larger values of $\kappa$. Figures 5–7, however, show a clear trend: the pressure drop

†Particles entering the channel form a relatively thick sediment layer which restricts the available area of clear liquid flow. This is the reason why the pressure drop of the channel increase distinctly for small $\kappa$.

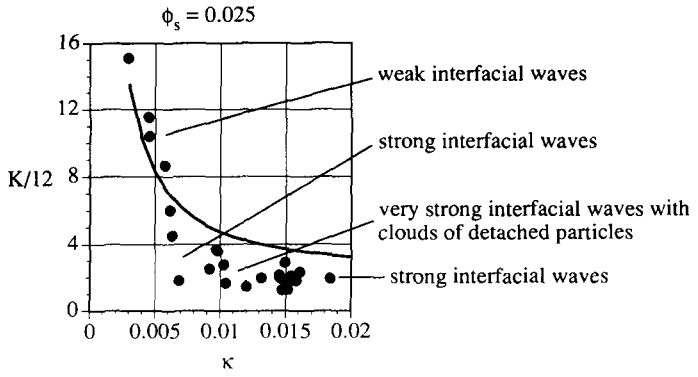


Figure 4. Measured pressure drop coefficient $K/12$ vs $\kappa$ for $0.02 < \phi_s < 0.03$ (water–ethanol mixture, $\rho_1 = 963\ \mathrm{kg/m^3}$; $\nu_1 = 2.86 \times 10^{-6}\ \mathrm{m^2/s}$; polystyrene beads with radius $a = 185\ \mu\mathrm{m}$ and density $\rho_2 = 1043\ \mathrm{kg/m^3}$) and comparison with theory (Schaflinger *et al.* 1990).

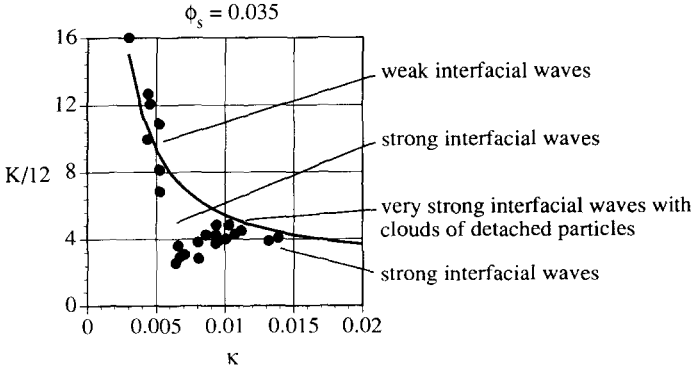


Figure 5. Measured pressure drop coefficient $K/12$ vs $\kappa$ for $0.03 < \phi_s < 0.04$ (water–ethanol mixture, $\rho_1 = 963\ \mathrm{kg/m^3}$; $\nu_1 = 2.86 \times 10^{-6}\ \mathrm{m^2/s}$; polystyrene beads with radius $a = 185\ \mu\mathrm{m}$ and density $\rho_2 = 1043\ \mathrm{kg/m^3}$) and comparison with theory (Schaflinger *et al.* 1990).

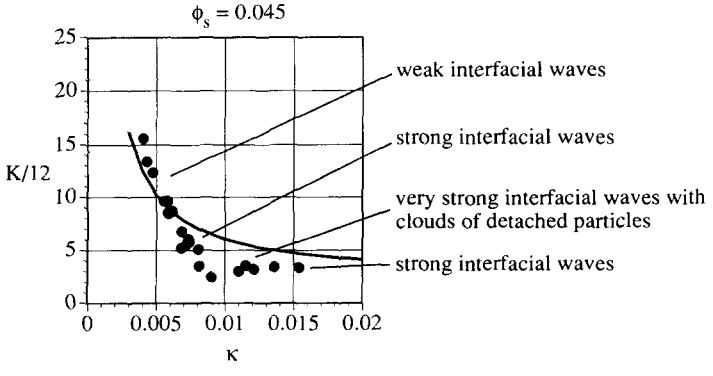


Figure 6. Measured pressure drop coefficient $K/12$ vs $\kappa$ for $0.04 < \phi_s < 0.05$ (water–ethanol mixture, $\rho_1 = 963\ \mathrm{kg/m^3}$; $\nu_1 = 2.86 \times 10^{-6}\ \mathrm{m^2/s}$; polystyrene beads with radius $a = 185\ \mu\mathrm{m}$ and density $\rho_2 = 1043\ \mathrm{kg/m^3}$) and comparison with theory (Schaflinger *et al.* 1990).

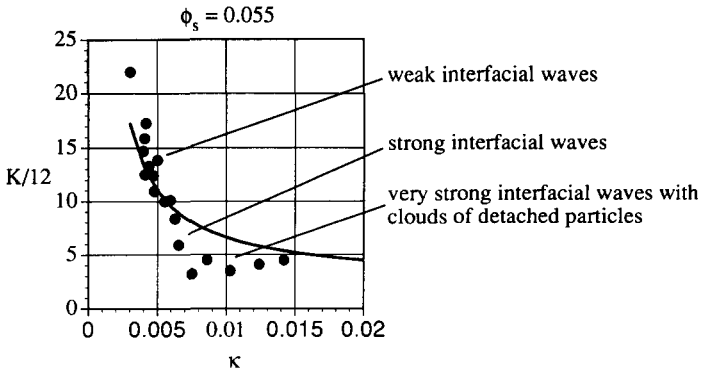


Figure 7. Measured pressure drop coefficient $K/12$ vs $\kappa$ for $0.05 < \phi_s < 0.06$ (water–ethanol mixture, $\rho_1 = 963\ \mathrm{kg/m^3}$; $\nu_1 = 2.86 \times 10^{-6}\ \mathrm{m^2/s}$; polystyrene beads with radius $a = 185\ \mu\mathrm{m}$ and density $\rho_2 = 1043\ \mathrm{kg/m^3}$) and comparison with theory (Schaflinger *et al.* 1990).

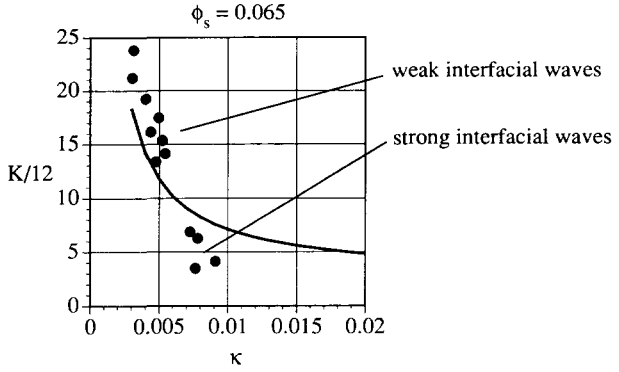


Figure 8. Measured pressure drop coefficient $K/12$ vs $\kappa$ for $0.06 < \phi_s < 0.07$ (water–ethanol mixture, $\rho_1 = 963\ \mathrm{kg/m^3}$; $\nu_1 = 2.86 \times 10^{-6}\ \mathrm{m^2/s}$; polystyrene beads with radius $a = 185\ \mu\mathrm{m}$ and density $\rho_2 = 1043\ \mathrm{kg/m^3}$) and comparison with theory (Schaflinger *et al.* 1990).

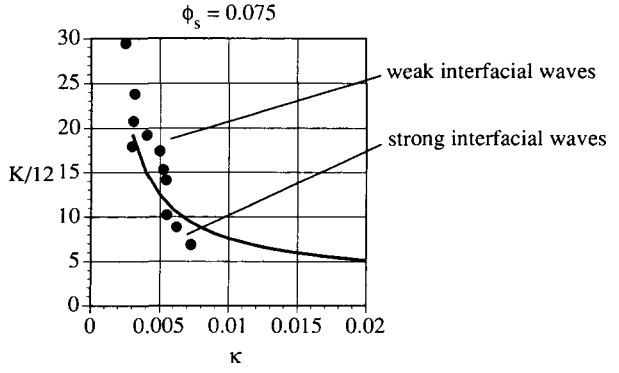


Figure 9. Measured pressure drop coefficient $K/12$ vs $\kappa$ for $0.07 < \phi_s < 0.08$ (water–ethanol mixture, $\rho_1 = 963\ \mathrm{kg/m^3}$; $\nu_1 = 2.86 \times 10^{-6}\ \mathrm{m^2/s}$; polystyrene beads with radius $a = 185\ \mu\mathrm{m}$ and density $\rho_2 = 1043\ \mathrm{kg/m^3}$) and comparison with theory (Schaflinger *et al.* 1990).

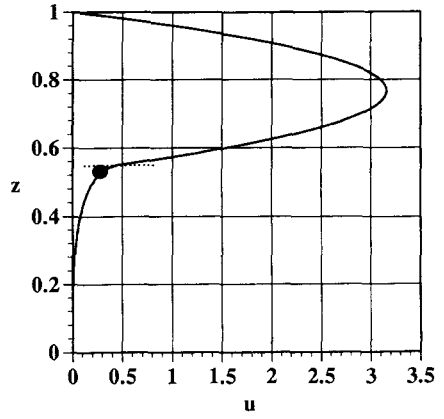


Figure 10. Measured interfacial velocity (●) and comparison with the theoretical velocity profile (solid line). The dotted line marks the position of the theoretically predicted interface. $\kappa = 0.004$, $\phi_s = 0.016$, $\rho_1 = 963\ \mathrm{kg/m^3}$, $\nu_1 = 2.86 \times 10^{-6}\ \mathrm{m^2/s}$ (water–ethanol mixture); $a = 185\ \mu\mathrm{m}$, $\rho_2 = 1043\ \mathrm{kg/m_3}$ (polystyrene beads).

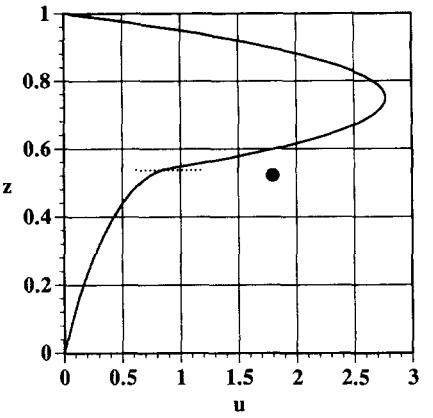


Figure 11. Measured interfacial velocity (●) and comparison with the theoretical velocity profile (solid line). The dotted line marks the position of the theoretically predicted interface. $\kappa = 0.01$, $\phi_s = 0.065$, $\rho_1 = 963\ \mathrm{kg/m^3}$, $\nu_1 = 2.86 \times 10^{-6}\ \mathrm{m^2/s}$ (water–ethanol mixture); $a = 185\ \mu\mathrm{m}$, $\rho_2 = 1043\ \mathrm{kg/m_3}$ (polystyrene beads).

coefficient always reached a minimum which coincides with the occurrence of very strong interfacial waves together with the creation of clouds of detached particles. Eventually, $K$ increased and attained a value almost independent of $\kappa$. Due to technical limitations we were unable to run experiments for $\phi_s > 0.06$ and larger $\kappa$.

Also we would like to mention that inertial life effects were always insignificant since in all cases the particle Reynolds number was below 0.15.

*(b) Measurements of the particle velocity at the interface*

By means of a mirror, the top view of the duct was recorded on a video together with the side view at the same time. Thus, it was possible to evaluate the particle velocities at the interface and to study the interfacial waves. Impurities on the particle-surface enabled us to track individual particles over a distance of several centimeters. For small values of the parameter $\kappa$, the experiments show that the particle velocity at the interface is in good agreement with that predicted theoretically (Schaflinger *et al.* 1990) even though slight interfacial instabilities were found to be present. Measurements for two different particle sizes are depicted in figures 10 and 12. It should be noted

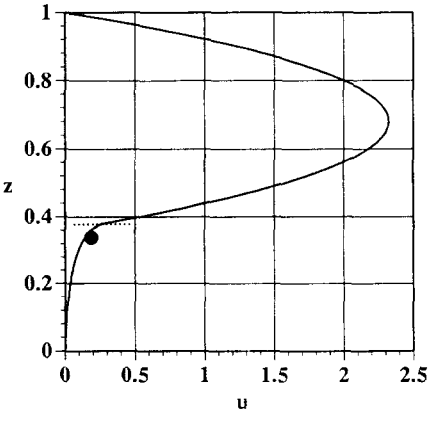


Figure 12. Measured interfacial velocity (●) and comparison with the theoretical velocity profile (solid line). The dotted line marks the position of the theoretically predicted interface. $\kappa = 0.008$, $\phi_s = 0.008$, $\rho_1 = 963\ \mathrm{kg/m^3}$, $\nu_1 = 2.86 \times 10^{-6}\ \mathrm{m^2/s}$ (water–ethanol mixture); $a = 410\ \mu\mathrm{m}$, $\rho_2 = 1031\ \mathrm{kg/m_3}$ (polystyrene beads).

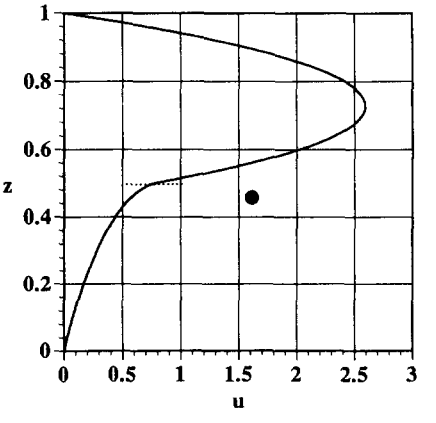


Figure 13. Measured interfacial velocity (●) and comparison with the theoretical velocity profile (solid line). The dotted line marks the position of the theoretically predicted interface. $\kappa = 0.012$, $\phi_s = 0.053$, $\rho_1 = 963\ \mathrm{kg/m^3}$, $\nu_1 = 2.86 \times 10^{-6}\ \mathrm{m^2/s}$ (water–ethanol mixture); $a = 410\ \mu\mathrm{m}$, $\rho_2 = 1031\ \mathrm{kg/m_3}$ (polystyrene beads).

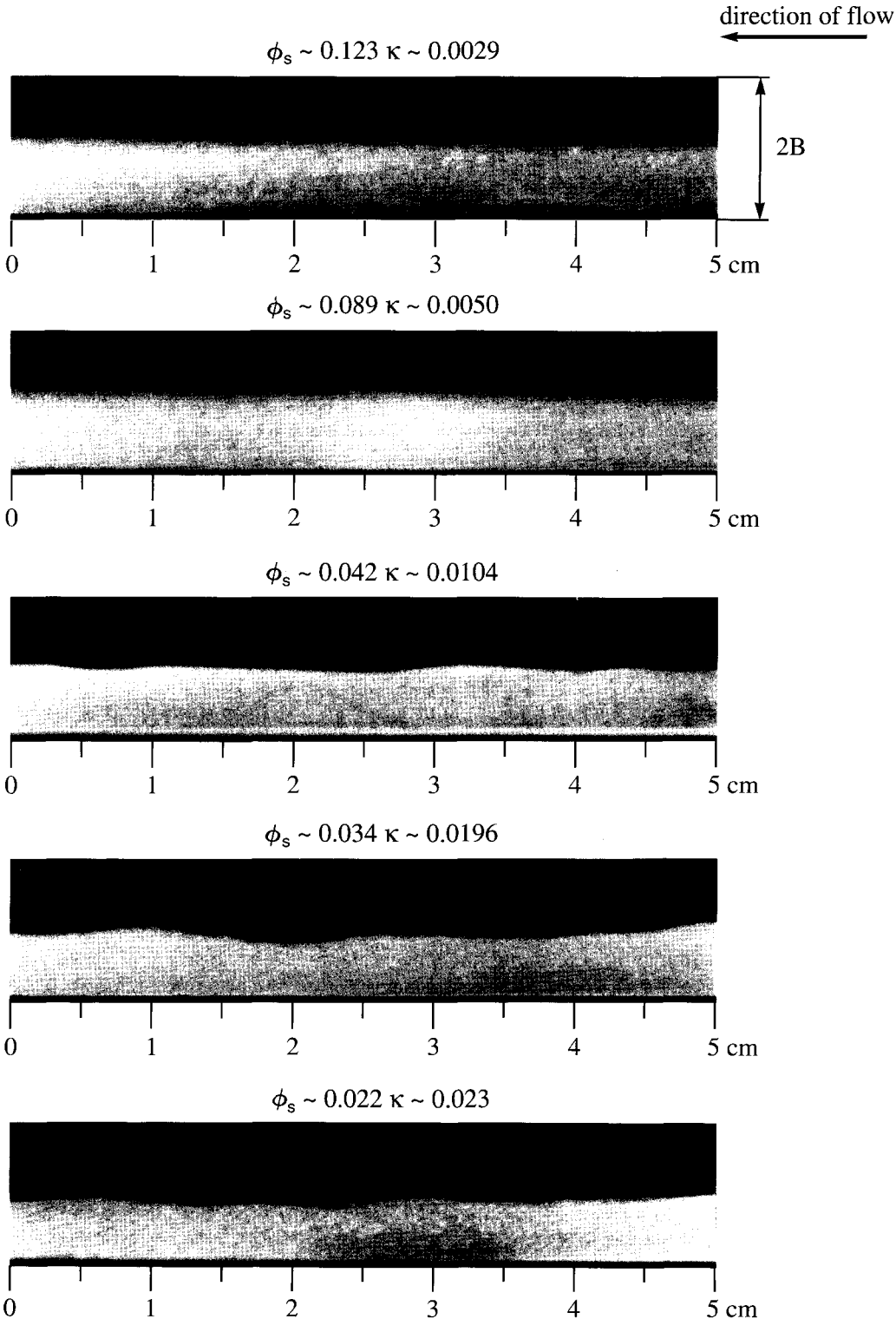


Figure 14. Side view of various resuspension experiments.

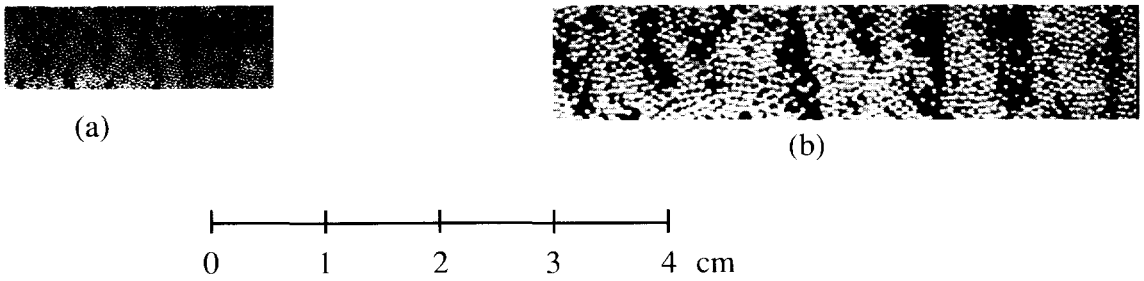


Figure 15. Top view of a ripple type instability for a monolayer of particles. $\kappa = 0.2$, $\rho_1 = 963\ \mathrm{kg/m^3}$, $\nu_1 = 2.86 \times 10^{-6}\ \mathrm{m^2/s}$ (water–ethanol mixture); (a) $a = 185\ \mu\mathrm{m}$; $\rho_2 = 1043\ \mathrm{kg/m_3}$ (polystyrene beads); (b) $a = 410\ \mu\mathrm{m}$, $\rho_2 = 1031\ \mathrm{kg/m^3}$ (polystyrene beads).

that the $z$ co-ordinate has been non-dimensionalized by the total spacing $2B$ and the velocity $u$ by $Q/2B$.

An increase in $\kappa$ led to particle velocities at the interface which were several times larger than those predicted by theory (figures 11 and 13). This was due to the fact that, since interfacial waves were very strong in this range of $\kappa$, particles were detached from the suspension and moved as a detached layer with rather a high speed.

*(c) Visual observations*

The existence of several different flow instabilities were noticed during the course of the experiments. First of all, the interface between the suspension and the clear liquid was found to be unstable throughout all the experimental runs and, in general, waves were observed with wavelengths comparable to the total spacing of the duct. Sometimes, however, at small values of $\kappa$, a rather weak long wave instability occurred with a wavelength in the order of 20 times the total spacing. In the range of $\kappa \sim 0.01$ both instabilities occasionally coexisted. This is consistent with the results of a linear stability analysis (Zhang *et al.* 1992; Schaflinger 1994) for the problem under investigation according to which weak long wave instabilities and strong short waves can coexist at the same time.

Figure 14 shows a sequence of side views of different experiments with $\kappa$ and $\phi_s$ being varied. In all cases, the interface between the suspension and the clear liquid was found to be unstable. However, as can be seen from the two top pictures (a and b), small values of $\kappa$ led to rather weak interfacial waves. Eventually, increasing $\kappa$ led to more vigorous instabilities with wave breaking and particles being detached (c and d). Finally, a further increase in $\kappa$ lessened wave destruction (e).

In the case of a monolayer of resuspended particles we observed a ripple type instability (figure 15). These waves set in at $\kappa \sim 0.04$ and had a wavelength which, surprisingly, did not change when $\kappa$ was increased up to 0.4. The measured wavelength was always approximately 10 particle diameters for both sizes of polystyrene beads with radius $a = 185\ \mu\mathrm{m}$ and $a = 410\ \mu\mathrm{m}$. To the best of the authors' knowledge nothing is known about the mechanism of such instabilities. The measured wave propagation velocity was relatively small and about 0.01 times $Q/2B$.

## 5. CONCLUSIONS

The purpose of this investigation was to compare experimental resuspension data with corresponding theoretical predictions for a fully developed laminar flow. Earlier measurements for the resuspension height $h_1$ (Leighton & Acrivos 1986; Schaflinger *et al.* 1990) showed large scatter which was mainly attributed to interfacial waves. Here we measured the pressure drop in a 2D Hagen–Poiseuille resuspension flow and compared the dimensionless pressure drop coefficient $K$ with theoretical values (Schaflinger *et al.* 1990). Such experiments are also of great practical interest since two-dimensional resuspension flow became recently very important in oil prospecting (Unwin & Hammond 1994).

The experiments were carried out in a set-up where both phases (solid particles of uniform size and density and the clear fluid) were continuously circulated. The concentration of the well-mixed

suspension was varied within the range $0 < \phi_s < 0.08$ and the Shields number was independently adjusted to lie between $0 < \kappa < 0.4$. Since a fully developed flow was usually reached within a short time, the pressure drop could easily be measured. The side and top views of the flowing system were recorded on a video in order to determine the particle velocities at the interface and to study interfacial instabilities.

The results show that the measured pressure drop coefficient $K$ was slightly larger than theoretically predicted (Schaflinger *et al.* 1990) for all cases if $\kappa$ was small. In this range, the particle velocities at the interface matched well with the theory even though weak interfacial waves were observed. Increasing the Shields number generated much stronger flow instabilities which introduced a significant scatter in the data if $\phi_s < 0.035$. However, for larger concentrations $\phi_s$ and increasing $\kappa$, the measured pressure drop coefficient $K$ decreased abruptly at $\kappa \sim 0.006$ and was found to be considerably lower than the corresponding theoretical value. It was also found from the experiments that $K$ attained a minimum just before vigorous interfacial waves caused wave breaking and the creation of clouds of detached particles flowing relatively rapidly above the original interface. Finally, it was observed, that with a further increase in $\kappa$, wave destruction lessened and $K$ increased.

We infer from the experiments that the discrepancy between theoretical predictions and experimental data is caused by flow instabilities. The pressure drop is related to the particle concentration within the resuspended layer. Interfacial waves certainly influence the concentration which causes the difference between the theoretical predictions for the pressure drop and the measurements. Only in the range of small $\kappa \sim 0.005$, which corresponds to a channel Reynolds number $\mathrm{Re} \sim 100$, did the measured interfacial velocities agree with those predicted by theory (Schaflinger *et al.* 1990). Zhang & Acrivos (1994) reported good agreement between their calculations and experimental results for a fully developed resuspension flow in a pipe with Reynolds numbers $\mathrm{Re} < 20$ as published by Altobelli *et al.* (1991).

In the limiting case of a monolayer of particles, a ripple type of instability was observed. The waves set in at $\kappa \sim 0.04$ and their wavelength was measured at about ten particle diameters which did not change while increasing flow rate of clear liquid, i.e. with increasing Shields number $\kappa$. To the best of the authors' knowledge the mechanism of this instability is not yet understood and subject for further investigation.

*Acknowledgements*—The authors are grateful to Dr J. Smart and H. Schulreich for their assistance in performing the experiments. The authors also thank Dr B. Kapoor for his constructive remarks. This research was supported in part by grants from the Austrian Science Foundation (P7909-TEC), the U.S. Department of Energy (DE-FG02-90-ER14139) and the National Science Foundation under the U.S.–Austrian Cooperative Program (INT-9012193).

## REFERENCES

Acrivos, A. 1993 The rheology of concentrated suspensions of non-colloidal particles. In *Particulate Two-phase flow* (Edited by Roco, M.). Butterworth–Heinemann, Boston, MA.

Altobelli, S. A., Givler, R. C. & Fukushima, E. 1991 Velocity and concentration measurements of suspensions by nuclear magnetic resonance imaging. *J. Rheol.* **35,** 721–734.

Borhan, A. 1988 Effects of concentration on the stability and efficiency of inclined super-settlers. Ph.D. thesis, Stanford University, CA.

Kapoor, B. & Acrivos, A. 1995 Flow of a sediment on an inclined plate. *J. Fluid Mech.* In press.

Leighton, D. & Acrivos, A. 1986 Viscous resuspension. *Chem. Engng Sci.* **41,** 1377–1384.

Leighton, D. & Acrivos, A. 1987a Measurement of shear-induced self-diffusion in concentrated suspensions of spheres. *J. Fluid Mech.* **177,** 109–131.

Leighton, D. & Acrivos, A. 1987b The shear-induced migration of particles in concentrated suspensions. *J. Fluid Mech.* **181,** 415–439.

Nir, A. & Acrivos, A. 1990 Sedimentation and sediment flow on inclined surfaces. *J. Fluid Mech.* **212,** 139–153.

Schaflinger, U., Acrivos, A. & Zhang, K. 1990 Viscous resuspension of a sediment within a laminar and stratified flow. *Int. J. Multiphase Flow* **16,** 567–578.

Schaflinger, U. 1994 Interfacial instabilities in a stratified of two superposed flow. *Fluid Dynam. Res.* **13,** 299–316.

Unwin, A. T. & Hammond, P. S. 1994 A simple phenomenological model for shear driven particle migration in concentrated viscoelastic suspension. *IUTAM Symposium on Liquid–Particle Interactions in Suspension Flow*, Grenoble, France.

Zhang, K., Acrivos, A. & Schaflinger, U. 1992 Stability in a two-dimensional Hagen–Poiseuille resuspension flow. *Int. J. Multiphase Flow* **18,** 51–63.

Zhang, K. & Acrivos, A. 1994 Viscous resuspension in fully developed pipe flow. *Int. J. Multiphase Flow* **20,** 579–591.